INTRACELLULAR TRAFFICKING PATHWAY OF YEAST LONG-CHAIN BASE KINASE LCB4, FROM ITS SYNTHESIS TO ITS DEGRADATION*

Soichiro Iwaki[‡1], Takamitsu Sano[‡1], Tomoko Takagi[§], Masako Osumi[¶‖], Akio Kihara[‡2], Yasuyuki Igarashi[‡]**

From the [‡]Laboratory of Biomembrane and Biofunctional Chemistry, Faculty of Pharmaceutical Sciences, Hokkaido University, Kita 12-jo, Nishi 6-choume, Kita-ku, Sapporo 060-0812, Japan, the [§]Division of Biology, Department of Life Sciences, Graduate School of Arts and Sciences, University of Tokyo, 3-8-1 Komaba, Meguro-ku, Tokyo 153-8902, Japan, the [¶]Laboratory of Electron Microscopy/Open Research Center, Japan Women's University, 2-8-1 Mejirodai, Bunkyo-ku, Tokyo 112-8681, Japan, the [‖]Non Profit Organization: Integrated Imaging Research Support, Villa Royal Hirakawa, 1-7-5, Hirakawacho, Chiyoda-ku Tokyo 102-0093, Japan, and the [**]Laboratory of Biomembrane and Biofunctional Chemistry, Faculty of Advanced Life Sciences, Hokkaido University, Kita 12-jo, Nishi 6-choume, Kita-ku, Sapporo 060-0812, Japan

Running title: Intracellular trafficking of Lcb4

Address correspondence to: Akio Kihara, Laboratory of Biomembrane and Biofunctional Chemistry, Faculty of Pharmaceutical Sciences, Hokkaido University, Kita 12-jo, Nishi 6-choume, Kita-ku, Sapporo 060-0812, Japan, Tel. +81-11-706-3971; Fax. +81-11-706-4986; E-mail: kihara@pharm.hokudai.ac.jp

Sphingoid long-chain base 1-phosphates (LCBPs) act as bioactive lipid molecules in eukaryotic cells. In budding yeast, LCBPs are synthesized mainly by the long-chain base kinase Lcb4. We recently reported that, soon after yeast cells enter into the stationary phase, Lcb4 is rapidly degraded by being delivered to the vacuole in a palmitoylation- and phosphorylation-dependent manner. In this study, we investigated the complete trafficking pathway of Lcb4, from its synthesis to its degradation. After membrane anchoring by palmitoylation at the Golgi apparatus, Lcb4 is delivered to the plasma membrane (PM) through the late Sec pathway and then to the endoplasmic reticulum (ER). The yeast ER consists of a cortical network juxtaposed to the PM (cortical ER) with tubular connections to the nuclear envelope (nuclear ER). Remarkably, the localization of Lcb4 is restricted to the cortical ER. As the cells reach the stationary phase, G_1 cell cycle arrest initiates Lcb4 degradation and its delivery to the vacuole via the Golgi apparatus. The protein transport pathway from the PM to the ER found in this study has not been previously reported. We speculate that this novel pathway is mediated by the PM-ER contact.

Sphingolipids are major constituents of eukaryotic plasma membranes. Ceramide, the structural backbone of sphingolipids, is generated from long-chain base (LCB)[3] and an amide-linked fatty acid. In addition, phosphorylation of the major mammalian LCB, sphingosine, by sphingosine kinase yields sphingosine 1-phosphate (S1P). By binding to receptors in the S1P/Edg family of G-protein-coupled receptors, S1P regulates various cellular processes including proliferation, differentiation, motility, and adherens junction assembly (1-4). In addition to its extracellular effects, S1P is thought to function as a second messenger of various stimuli, such as growth factors and cytokines, and to elicit cellular responses including Ca^{2+} mobilization and apoptosis inhibition (1, 2, 4).

The yeast *Saccharomyces cerevisiae* does not contain S1P, but instead has two other long-chain base 1-phosphates (LCBPs), dihydrosphingosine 1-phosphate and phytosphingosine 1-phosphate. The synthesis and metabolic pathways of LCBPs are highly conserved between mammalian and yeast cells, and yeast LCBPs are produced by LCB kinases that correspond to mammalian sphingosine kinases. Yeast have two LCB kinases, Lcb4 and Lcb5, although Lcb4 is responsible for most cellular activity. Yeast cells, however, do not have cell surface receptors for LCBPs, so these compounds function only intracellularly. Similar to the intracellular functions of S1P in mammals, LCBPs in yeast are involved in diverse cellular processes including heat stress resistance and Ca^{2+} mobilization (5-8).

Recently, we found that the stability and

localization of Lcb4 were regulated by its post-translational modifications, including palmitoylation, phosphorylation, and ubiquitination (9, 10). Palmitoylation of Lcb4 is catalyzed by the palmitoyltransferase Akr1, while Pho85 cyclin-dependent kinase is responsible for its phosphorylation. Interestingly, the phosphorylation of Lcb4 is greatly reduced in Δ*akr1* cells (10), suggesting that the palmitoylation is a prerequisite for the phosphorylation. Palmitoylation is also involved in the membrane anchoring of Lcb4, which otherwise would be a soluble protein. Although Lcb4 is relatively stable in the log phase of cell growth, it is destabilized upon the cell reaching the stationary phase. Both palmitoylation and phosphorylation are required during the stationary phase for the degradation of Lcb4, which is delivered to the vacuole via the multivesicular body (MVB), then degraded (9, 10).

In a previous report, we demonstrated that in log phase Lcb4 is localized primarily in the endoplasmic reticulum (ER), although it is also found in the plasma membrane (PM) (11). However, it was unclear how Lcb4 reaches the ER or PM. In the present study, we investigated the complete trafficking pathway of Lcb4, from its synthesis to its degradation. We found that localization of Lcb4 in the ER was unusually restricted to the cortical ER. In addition, our results strongly support the existence of a novel PM-to-ER transport pathway. Transport of Lcb4 via the PM-ER contact site is an intriguing possibility that would also explain its unique, cortical ER-specific localization.

Experimental Procedures

Yeast Strains and Media – *S. cerevisiae* strains used in this study are listed in Table 1. For construction of the Δ*pep12::LEU2* cells, the 0.56 kb *Bgl*II-*Kpn*I region of the *PEP12* gene was replaced with the *LEU2* marker. TS335 cells were prepared by backcrossing HMSF1 (*sec1-1*) cells with cells of the SEY6210 background strain four times.

Cells were grown either in YPD medium (1% yeast extract, 2% peptone, and 2% glucose) or in synthetic complete medium (SC; 0.67% yeast nitrogen base and 2% glucose) containing nutritional supplements. To synchronize the growth of the cells in culture, rapamycin (200 ng/ml), α-factor (6 μg/ml), nocodazole (15 μg/ml), or hydroxyurea (100 mM) was added to the medium.

Plasmids – The centromere-based (*CEN*) low-copy-number plasmid pRS313 (*HIS3* marker) (12), and the 2 μ-based high-copy-number plasmids pRS423 (*HIS3* marker) and pRS426 (*URA3* marker) (13) were used as vectors. The pWK78 (*LCB4, CEN*, *HIS3* marker) and pWK79 (*LCB4,* 2 μ, *HIS3* marker) plasmids were derived from the pRS313 and pRS423 plasmids, respectively, as described previously (9). The pWK81 (*LCB4,* 2 μ, *URA3* marker) was constructed by cloning the 3.0-kb *Bam*HI-*Sal*I fragment of pWK79 into the *Bam*HI-*Sal*I sites of pRS426.

The plasmid pUG34, a yeast expression vector encoding a fusion protein with an N-terminal enhanced green fluorescent protein (EGFP) under the control of the *MET15* promoter, was a gift from Dr. J. H. Hegemann (Heinrich-Heine University, Düsseldorf, Germany). The pWK63 (*MET15* promoter, *EGFP-LCB4, CEN, HIS3* marker) plasmid was described previously (9).

Immunoblotting – Immunoblotting was performed as described previously (14), using ECL™ or ECL Plus™ Western blotting detection reagents (GE Healthcare Bio-Sciences, Piscataway, NJ). Affinity-purified anti-Lcb4 antibodies (1:1,000 dilution) (9), anti-Dpm1 (dolichol phosphate mannose synthase) antibodies (2 μg/ml; Invitrogen), and anti-Pma1 (plasma membrane proton ATPase) antibodies (0.4 μg/ml; Santa Cruz Biotechnology, Santa Cruz, CA) were used as primary antibodies. Peroxidase-conjugated donkey anti-rabbit IgG $F(ab')_2$ and sheep anti-mouse IgG $F(ab')_2$, each diluted at 1:10,000 (GE Healthcare Bio-Sciences), and peroxidase-conjugated donkey anti-goat IgG (0.08 μg/ml; Santa Cruz Biotechnology) were used as secondary antibodies.

Fluorescence Microscopy – Immunofluorescence

microscopy was performed as described previously (14). Anti-Pma1 antibodies (8 μg/ml) and anti-Kar2 antiserum (1:200 dilution; a gift from Dr. Yoshihisa, Nagoya University, Nagoya, Japan) were used as primary antibodies. Alexa Fluor 488-conjugated goat anti-rabbit IgG(H+L) and donkey anti-goat IgG(H+L) antibodies (each at 6.7 μg/ml; Invitrogen) were used as secondary antibodies. Lcb4 was detected using affinity-purified anti-Lcb4 antibodies (9) that had been pre-incubated with SIY03 (Δ*lcb4*) cell lysates to reduce nonspecific background and directly labeled using a Zenon™ Alexa Fluor 594 Rabbit IgG labeling kits (Invitrogen), according to the manufacturer's instructions.

Microscopic EGFP-fluorescence was performed as described previously (9). Cells were analyzed by fluorescence microscopy using an Axioskop 2 PLUS microscope (Carl Zeiss, Oberkochen, Germany)

Immunoelectron microscopy – High-pressure freezing and freeze-substitution of yeast cells were performed as described previously (15, 16). Immunoelectron microscopy was performed as described previously (17) with affinity-purified anti-Lcb4 antibodies (1:1,000 dilution) and 10 nm colloidal gold-conjugated goat anti-rabbit IgG (1:40 dilution; British BioCell, UK). The stained cells were examined using a transmission electron microscope JEM 1200 EXS (JEOL Ltd., Tokyo, Japan) at 80 kV.

Sucrose gradient fractionation – Sucrose gradient fractionation was performed as described previously (18). Briefly, approximately 5 x 10^8 cells were converted to spheroplasts and lysed in a 12.5% sucrose solution in buffer I (20 mM HEPES-NaOH (pH 7.5), 10 mM EDTA, 1 x protease inhibitor mixture (Complete™; Roche Diagnostics, Indianapolis, IN), 1 mM phenylmethylsulfonyl fluoride, and 1 mM dithiothreitol). After removal of cell debris by centrifugation, total lysates (0.425 ml) were overlaid onto a discontinuous sucrose gradient (0.319 ml of 26%, 0.319 ml of 34%, 0.638 ml of 42%, 1.275 ml of 46%, 0.85 ml of 50%, 0.638 ml of 54%, and 0.425 ml of 60% sucrose (w/v) in buffer I), and the samples were centrifuged at 235,000 x *g* for 4 h. Fractions were collected from the top and separated by SDS-PAGE, followed by immunoblotting.

Pulse-chase and immunoprecipitation – Pulse-chase experiments and subsequent immunoprecipitation were performed as described previously (9). Briefly, yeast cells were grown to early log phase at 30˚C in SC medium lacking methionine and cysteine. Cells were pulse-labeled for 15 min with [^{35}S]methionine/[^{35}S]cysteine (EXPRESS™ Protein Labeling Mix; 1,000 Ci/mmol; PerkinElmer) at 25 μCi per 10^7 cells, then chased with cold methionine (final concentration 0.5 mg/ml) and cysteine (final concentration 0.1 mg/ml) for the indicated time periods. Cell lysates were prepared as described previously (14), and Lcb4 was then immunoprecipitated using anti-Lcb4 antiserum (9) and protein A-sepharose beads (GE Healthcare Bio-Sciences). Samples were separated by SDS-PAGE, and the gels were fixed, treated with the Amplify Fluorographic Reagent™ (GE Healthcare Bio-Sciences), dried, and exposed to X-ray film at -80˚C.

RESULTS

Lcb4 is localized in the cortical ER – We first examined the localization of Lcb4 by indirect immunofluorescence microscopy using anti-Lcb4 antibodies. A weak signal was detected near the cell surface in wild-type cells, but was not observed in Δ*lcb4* cells (Fig. 1*A*). In cells in which Lcb4 was produced from a 2 μ plasmid, cell surface staining became more prominent (Fig. 1*A*), agreeing with our previous result (10).

We also investigated the localization of Lcb4 by sucrose density gradient. As previously reported (11), endogenous Lcb4 was localized mainly in the ER fractions but partly in the PM fractions (Fig. 1*B*). When Lcb4 was expressed from a *CEN* plasmid, its subcellular localization was almost the same as that observed in wild-type cells (Fig. 1*C*).

In fluorescence microscopy, yeast ER typically appear as two ring structures, the nuclear ER

and the cortical ER, as demonstrated by the staining patterns of the ER protein Kar2 (Fig. 1*A*). However, the cortical ER is closely adjacent to the PM, identified by its marker Pma1 (Fig. 1*A*), so immunofluorescence cannot distinguish between the two. Sucrose density gradient separation revealed that most of the endogenous Lcb4 was localized in the ER (Fig. 1*B*), although no nuclear ER-staining was observed (Fig. 1*A*). These results suggest that the ER localization of Lcb4 is restricted to the cortical ER and that the cell surface staining observed corresponds to both the PM and the cortical ER.

To confirm the cortical ER localization of Lcb4, we investigated endogenous and overproduced Lcb4 by immunoelectron microscopy. As presented in Fig. 2*A*, the ER structures were distinguishable as characteristic transparent structures (19) that included the cortical ER (closed arrows) and the nuclear ER (open arrows). Overproduced Lcb4 was indeed detected in the cortical ER (closed arrowheads) but not in the nuclear ER (Fig. 2*B*). Plasma membrane localization was also observed in some cells (data not shown). Similarly, endogenous Lcb4 was observed in the cortical ER (Fig. 2*C*) but not in the nuclear ER. These results indicate that Lcb4 is indeed localized specifically in the cortical ER.

Lcb4 is transported to the PM via the Golgi apparatus – Recently, we demonstrated that Lcb4 is anchored to the membrane through its palmitoylation by the palmitoyltransferase Akr1 (10). Considering that Akr1 is predominantly localized in the Golgi apparatus (20), we speculated that Lcb4 is transported to the PM/ER after being palmitoylated at the Golgi apparatus. To test this theory, we prepared an EGFP-Lcb4 construct under the control of the inducible *MET15* promoter, which enabled us to monitor only the newly-synthesized EGFP-Lcb4. We introduced this construct into wild-type or *sec1-1* temperature-sensitive mutants, in which the late Sec pathway involved in vesicular transport from the Golgi apparatus to the PM is abolished at restrictive temperatures (37˚C). In wild-type cells grown at either 23˚C or 37˚C, EGFP-Lcb4 was observed at the cell periphery. In contrast, in the *sec1-1* mutants EGFP-Lcb4 was distributed in punctate structures characteristic of the Golgi apparatus, at the restrictive temperature (37˚C) but not at the permissive temperature (23˚C) (Fig. 3*A*). This result indicates that Golgi-to-PM transport via the late Sec pathway is essential not only for the PM localization but also for the cortical ER localization of Lcb4. Thus, it is highly likely that Lcb4 is transported to the ER after reaching the PM.

To determine the site of Lcb4 phosphorylation, we next examined the phosphorylation in *sec1-1* mutants over time using a pulse-chase experiment. Lcb4 was gradually converted to its phosphorylated form in wild-type cells at either temperature, and in the *sec1-1* mutants at the permissive temperature (Fig. 3*B*). On the other hand, almost no phosphorylation was observed in *sec1-1* mutants at the restrictive temperature. These results indicate that Lcb4 is phosphorylated after reaching the PM.

Lcb4 is transported from the ER to the vacuole via the Golgi/MVB in the stationary phase – Previously, we demonstrated that upon reaching the stationary phase, Lcb4 is rapidly delivered via the MVB to the vacuole for degradation (9). However, it is unclear how the Lcb4, localized in the ER during the log phase, is transported to the MVB/vacuole. One possibility is that Lcb4 is transported from the ER to the Golgi apparatus via vesicular transport (early Sec pathway) and then to the MVB/vacuole. Or, perhaps Lcb4 returns to the PM and is transported to the MVB/vacuole via endocytosis. To distinguish between these possibilities, we investigated the degradation of Lcb4 in early *sec* and endocytosis mutants. The temperature-sensitive mutants *sec12-1* and *sec23-1* carry mutations in the component of the COPII complex that is involved in the transport from the ER to the Golgi apparatus. Cells were cultured until just before entering the stationary phase, then were shifted to the restrictive temperature. Although it was degraded in a time-dependent manner in wild-type cells, Lcb4 was not degraded in either the *sec12-1* or *sec23-1* mutants (Fig. 4*A*), indicating that Lcb4 is indeed transported from the ER to the Golgi via the early Sec pathway. On the other hand, mutations affecting endocytosis (Δ*sla1*, Δ*chc1*, and

Δ*clc1*) did not affect the stability of Lcb4, confirming that it is not transported to the vacuole via the endocytosis pathway (Fig. 4*B*). These results also support the existence of a PM-to-ER transport pathway, since the PM-localized Lcb4 must be delivered to the ER prior to its degradation.

Next, we examined the stability of Lcb4 using deletion mutants with defective post-Golgi transport. As shown in Fig. 4*C*, the stability of Lcb4 during the stationary phase was increased in mutants carrying deletions (Δ*vps45* and Δ*pep12*) that affect the SNARE complex, which is involved in transport between the Golgi apparatus and the MVB. We also examined the localization of EGFP-Lcb4 in log and stationary phases in these mutants. In wild-type cells EGFP-Lcb4 was observed near the cell surface in the log phase, whereas vacuolar staining was evident in the stationary phase, reflecting the accumulation of the stable EGFP moiety (Fig. 4*D*). On the other hand, EGFP-Lcb4 was observed in intracellular organelles in both Δ*vps45* and Δ*pep12* cells at the stationary phase (Fig. 4*D*). These results indicate that Lcb4 is transported from the ER to the vacuole via the Golgi/MVB at the stationary phase.

G_1 cell cycle arrest accelerates the degradation of Lcb4 – Yeast cells in glucose-containing medium proliferate by fermenting glucose, but the exhaustion of glucose causes a conversion in metabolism from fermentation to respiration, which utilizes ethanol. This conversion is called the diauxic shift. After yeast cells reach the diauxic shift, they undergo G_1 cell cycle arrest and enter into the stationary phase. To test whether the degradation of Lcb4 at the stationary phase is related to the G_1 cell cycle arrest, we examined the stability of Lcb4 in cultures treated with drugs that synchronize the cells at the G_1 phase. Rapamycin inhibits Tor kinase and arrests the cell cycle at the G_1 phase (21, 22). Treatment with 200 ng/ml rapamycin resulted in the stimulation of Lcb4 degradation (Fig. 5*A*). The mating pheromone α-factor similarly arrests the cell cycle in the late G_1 phase. Since exogenous α-factor is degraded rapidly by the secreted protease Bar1 (23), we used Δ*bar1* cells. Treatment with 6 μg/ml α-factor resulted in enhanced Lcb4 degradation (Fig. 5*B*). In contrast, treatment with 15 μg/ml nocodazole, which inhibits the polymerization of tubulin molecules and arrests cells at the M phase, or with 100 mM hydroxyurea, which inhibits ribonucleotide reductase and arrests cells at the S phase, did not affect the stability of Lcb4 (Fig. 5*A*). These results indicate that G_1 cell cycle arrest causes stimulation of Lcb4 degradation.

DISCUSSION

There have been discrepancies among studies as to the intracellular localization of Lcb4. Using indirect immunofluorescence microscopy, we detected non-tagged Lcb4 near the cell surface, regardless of its expression level (Fig. 1*A*; ref. 10). However, two other groups obtained different results using C-terminally HA-tagged Lcb4 (Lcb4-HA) expressed at the endogenous level. One group detected Lcb4-HA as a punctate pattern and diffuse patches, which overlapped with the Golgi and endosome markers (24). The other group observed punctate staining as well, but also a ring-like staining, which co-localized with an ER marker (25). We considered that these differences might be caused by the C-terminal tag. In fact, we observed punctate structures when examining the localization of overproduced Lcb4-HA (data not shown), confirming that the C-terminal tag does indeed affect the intracellular localization of Lcb4. In contrast, the observed ER localization is quite reasonable, since the substrates of Lcb4, LCBs, are synthesized in the ER. PM localization has also been expected, since exogenously added LCBs are converted in the PM to LCBPs to be utilized as sphingolipid precursors (26-28).

The ER of the budding yeast *Saccharomyces cerevisiae* appears as two simple rings, the cortical ER juxtaposed with the PM and the nuclear ER equivalent to the nuclear envelope. The cortical ER is a network of highly dynamic tubules that undergo ring closure and tubule-branching movements, similar to the mammalian peripheral ER (29). The cortical-specific ER localization we observed for Lcb4 is unusual (Figs. 1 and 2), however similar localization has been reported for other ER proteins such as Rtn1 and Rtn2

(30).

We also identified the complete intracellular trafficking pathways of Lcb4, from synthesis to degradation, as illustrated in Fig. 6. Since Lcb4 has no signal sequence or transmembrane domain, it must be synthesized in the cytosol and anchored to the Golgi apparatus through palmitoylation by Akr1. Lcb4 is then delivered to the PM via the late Sec pathway and then to the ER. Lcb4 is degraded slowly during the log phase, but its degradation is accelerated at the stationary phase. For degradation, Lcb4 is delivered from the ER to the Golgi via the early Sec pathway, then finally to the vacuole through the MVB.

Transport from the PM to the ER has been reported for lipid molecules such as sterols and fatty acids (31, 32), although the molecular mechanism is mostly unknown. Recently, however, a role for the ATP binding cassette transporters Aus1 and Pdr11 in ergosterol transport from the PM to the ER was reported (33). In contrast, PM-to-ER transport has not been established for proteins. At present, the mechanism responsible for transporting Lcb4 from the PM to the ER is unclear. However, since recent studies revealed that the ER is in contact with various organelles, such as the mitochondria, the PM, the *trans*-Golgi network, the endosome, and the vacuole (34-37), we speculate that the PM-ER contact may be responsible for the Lcb4 transport. Yeast cortical ER has been shown to be associated with the PM at a site called the PM-associated membrane (PAM) (36, 38, 39). The unique, cortical ER-specific localization of Lcb4 can be nicely explained by its hypothesized transport via the PAM. Since the PM contacts the cortical ER only at the PAM, Lcb4 is supplied to the cortical ER but not to the nuclear ER in this model. The cortical ER is connected with the nuclear ER via the tubular structure (29), so diffusion of Lcb4 to the nuclear ER via the tubules may be possible. However, considering the much larger area of the cortical ER, as compared to that of the tubules, it is highly likely that diffusion within the cortical ER would surpass that to the nuclear ER.

Reportedly, the PAM is enriched in several lipid biosynthetic enzymes (31, 40), implying that it contains a characteristic lipid composition (40). We recently reported that the transport of Lcb4 to the ER is influenced by the lipid environment (11). The localization of Lcb4 in the PM is greatly reduced in ergosterol biosynthetic mutants (11), suggesting that the PM-to-ER transport is accelerated in these mutants.

Until now, the components of the contact sites between the ER and other organelles have remained almost unknown. However, recent studies in yeast have revealed that the contact site between the nuclei and the vacuole, which is called a nucleus-vacuole junction, is formed by the interaction of the nuclear ER protein Nvj1 with the vacuolar protein Vac8 (31, 35-37). This suggests that a protein-protein interaction is responsible for the formation of contact sites between the ER and other organelles.

Disruption of the *ICE2* gene, which encodes a novel ER membrane protein, reportedly results in a defect in the delivery of ER into daughter cells (41). In addition, the cortical ER of Δ*ice2* cells is less continuous in the mother cell as compared to that in wild-type cells (41). However, our sucrose density gradient fractionation studies demonstrated the subcellular localization of Lcb4 in Δ*ice2* cells to be almost the same as in wild-type cells (our unpublished data). Furthermore, deletion of the *ICE2* gene had no apparent effect on the LCB kinase activity (our unpublished data). Thus, in Δ*ice2* cells Lcb4 is delivered to the ER. The cortical ER does still exist in Δ*ice2* cells (41), and this may account for the ineffectiveness of the *ICE2* deletion on Lcb4 localization and activity.

In the study presented here, G_1 arrest by inhibitors of cell cycle progression (rapamycin and α-factor) promoted the degradation of Lcb4 (Fig. 5). The exact molecular mechanism by which Lcb4 was degraded, however, remains unclear. We speculate that modification of Lcb4 is involved. We previously reported (9) that Lcb4 is phosphorylated by the cyclin-dependent kinase Pho85 complexed with the G_1 cyclin Pcl1/Pcl2, which are activated at the G_1 phase (42, 43). This phosphorylation is indeed required, but is not sufficient, for the degradation of Lcb4. We also demonstrated that Lcb4 is ubiquitinated, and that the phosphorylation functions to increase the efficiency of the ubiquitination (9). It is possible that

the ubiquitin ligase acting on Lcb4 is activated under G_1 cell cycle-arrested conditions.

The down-regulation of Lcb4 in the G_1 phase is considered to be important in regulating the cellular levels of LCBs and LCBPs. Interestingly, LCBs are required for transient cell cycle arrest induced by heat shock, and cell cycle recovery from this transient arrest is repressed in Δ*lcb4* Δ*lcb5* cells (44). Thus, it is possible that LCBPs are involved in G_1-to-S phase progression. A similar function has also been proposed for the mammalian LCBP, S1P. Increasing intracellular S1P levels following the overexpression of SPHK1, a homologue of Lcb4, results in a decreased number of cells in G_1/G_0-phase and an increase in those in S-phase, under normal and low serum conditions (45). Therefore, down-regulation of Lcb4 in G_1 phase may be important for maintenance of G_1 cell cycle arrest.

Our results suggest the existence of a novel trafficking pathway from the PM to the ER. Recently, it was reported that certain proteins, such as the GTPase Ras2 and the eight-transmembrane protein Ist2, traffic from the ER to the PM via a Sec-independent pathway (46, 47). Although the molecular mechanisms behind the transport of these proteins are unknown, the transport of Ras2 and Ist2 via the PAM is an intriguing possibility, as in the case of Lcb4. To test this possibility, identification of proteins involved in the formation of the PAM will be necessary.

REFERENCES

1. Pyne, S., and Pyne, N. J. (2000) *Biochem. J.* **349**, 385-402
2. Spiegel, S., and Milstien, S. (2003) *Nat. Rev. Mol. Cell Biol.* **4**, 397-407
3. Taha, T. A., Argraves, K. M., and Obeid, L. M. (2004) *Biochim. Biophys. Acta* **1682**, 48-55
4. Kihara, A., Mitsutake, S., Mizutani, Y., and Igarashi, Y. (2007) *Prog. Lipid Res.* **46,** 126-144
5. Mandala, S. M., Thornton, R., Tu, Z., Kurtz, M. B., Nickels, J., Broach, J., Menzeleev, R., and Spiegel, S. (1998) *Proc. Natl. Acad. Sci. U. S. A.* **95**, 150-155
6. Mao, C., Saba, J. D., and Obeid, L. M. (1999) *Biochem. J.* **342**, 667-675
7. Skrzypek, M. S., Nagiec, M. M., Lester, R. L., and Dickson, R. C. (1999) *J. Bacteriol.* **181**, 1134-1140
8. Birchwood, C. J., Saba, J. D., Dickson, R. C., and Cunningham, K. W. (2001) *J. Biol. Chem.* **276**, 11712-11718
9. Iwaki, S., Kihara, A., Sano, T., and Igarashi, Y. (2005) *J. Biol. Chem.* **280**, 6520-6527
10. Kihara, A., Kurotsu, F., Sano, T., Iwaki, S., and Igarashi, Y. (2005) *Mol. Cell. Biol.* **25**, 9189-9197
11. Sano, T., Kihara, A., Kurotsu, F., Iwaki, S., and Igarashi, Y. (2005) *J. Biol. Chem.* **280**, 36674-36682
12. Sikorski, R. S., and Hieter, P. (1989) *Genetics* **122**, 19-27
13. Christianson, T. W., Sikorski, R. S., Dante, M., Shero, J. H., and Hieter, P. (1992) *Gene* **110**, 119-122
14. Kihara, A., and Igarashi, Y. (2002) *J. Biol. Chem.* **277**, 30048-30054
15. Konomi, M., Kamasawa, N., Takagi, T., and Osumi, M. (2000) *Plant Morphology* **12**, 20-31
16. Humbel, B. M., Konomi, M., Takagi, T., Kamasawa, N., Ishijima, S. A., and Osumi, M. (2001) *Yeast* **18**, 433-444
17. Takagi, T., Ishijima, S. A., Ochi, H., and Osumi, M. (2003) *J. Electron Microsc. (Tokyo)* **52**, 161-174
18. Kihara, A., and Igarashi, Y. (2004) *Mol. Biol. Cell* **15**, 4949-4959
19. Preuss, D., Mulholland, J., Kaiser, C. A., Orlean, P., Albright, C., Rose, M. D., Robbins, P. W., and Botstein, D. (1991) *Yeast* **7**, 891-911
20. Roth, A. F., Feng, Y., Chen, L., and Davis, N. G. (2002) *J. Cell Biol.* **159**, 23-28
21. Heitman, J., Movva, N. R., and Hall, M. N. (1991) *Science* **253**, 905-909
22. Kunz, J., Henriquez, R., Schneider, U., Deuter-Reinhard, M., Movva, N. R., and Hall, M. N. (1993) *Cell* **73**, 585-596
23. MacKay, V. L., Welch, S. K., Insley, M. Y., Manney, T. R., Holly, J., Saari, G. C., and Parker, M. L.

(1988) *Proc. Natl. Acad. Sci. U. S. A.* **85**, 55-59
24. Hait, N. C., Fujita, K., Lester, R. L., and Dickson, R. C. (2002) *FEBS Lett.* **532**, 97-102
25. Funato, K., Lombardi, R., Vallee, B., and Riezman, H. (2003) *J. Biol. Chem.* **278**, 7325-7334
26. Mao, C., Wadleigh, M., Jenkins, G. M., Hannun, Y. A., and Obeid, L. M. (1997) *J. Biol. Chem.* **272**, 28690-28694
27. Qie, L., Nagiec, M. M., Baltisberger, J. A., Lester, R. L., and Dickson, R. C. (1997) *J. Biol. Chem.* **272**, 16110-16117
28. Mao, C., and Obeid, L. M. (2000) *Methods Enzymol.* **311**, 223-232
29. Prinz, W. A., Grzyb, L., Veenhuis, M., Kahana, J. A., Silver, P. A., and Rapoport, T. A. (2000) *J. Cell Biol.* **150**, 461-474
30. Voeltz, G. K., Prinz, W. A., Shibata, Y., Rist, J. M., and Rapoport, T. A. (2006) *Cell* **124**, 573-586
31. Levine, T. (2004) *Trends Cell Biol.* **14**, 483-490
32. Baumann, N. A., Sullivan, D. P., Ohvo-Rekilä, H., Simonot, C., Pottekat, A., Klaassen, Z., Beh, C. T., and Menon, A. K. (2005) *Biochemistry* **44**, 5816-5826
33. Li, Y., and Prinz, W. A. (2004) *J. Biol. Chem.* **279**, 45226-45234
34. Staehelin, L. A. (1997) *Plant J.* **11**, 1151-1165
35. Pan, X., Roberts, P., Chen, Y., Kvam, E., Shulga, N., Huang, K., Lemmon, S., and Goldfarb, D. S. (2000) *Mol. Biol. Cell* **11**, 2445-2457
36. Voeltz, G. K., Rolls, M. M., and Rapoport, T. A. (2002) *EMBO Rep.* **3**, 944-950
37. Kvam, E., Gable, K., Dunn, T. M., and Goldfarb, D. S. (2005) *Mol. Biol. Cell* **16**, 3987-3998
38. Baumann, O., and Walz, B. (2001) *Int. Rev. Cytol.* **205**, 149-214
39. Du, Y., Ferro-Novick, S., and Novick, P. (2004) *J. Cell Sci.* **117**, 2871-2878
40. Pichler, H., Gaigg, B., Hrastnik, C., Achleitner, G., Kohlwein, S. D., Zellnig, G., Perktold, A., and Daum, G. (2001) *Eur. J. Biochem.* **268**, 2351-2361
41. Estrada de Martin, P., Du, Y., Novick, P., and Ferro-Novick, S. (2005) *J. Cell Sci.* **118**, 65-77
42. Espinoza, F. H., Ogas, J., Herskowitz, I., and Morgan, D. O. (1994) *Science* **266**, 1388-1391
43. Measday, V., Moore, L., Ogas, J., Tyers, M., and Andrews, B. (1994) *Science* **266**, 1391-1395
44. Jenkins, G. M., and Hannun, Y. A. (2001) *J. Biol. Chem.* **276**, 8574-8581
45. Olivera, A., Kohama, T., Edsall, L., Nava, V., Cuvillier, O., Poulton, S., and Spiegel, S. (1999) *J. Cell Biol.* **147**, 545-558
46. Dong, X., Mitchell, D. A., Lobo, S., Zhao, L., Bartels, D. J., and Deschenes, R. J. (2003) *Mol. Cell Biol.* **23**, 6574-6584
47. Jüschke, C., Wächter, A., Schwappach, B., and Seedorf, M. (2005) *J. Cell Biol.* **169**, 613-622
48. Robinson, J. S., Klionsky, D. J., Banta, L. M., and Emr, S. D. (1988) *Mol. Cell. Biol.* **8**, 4936-4948
49. Kaiser, C. A., and Schekman, R. (1990) *Cell* **61**, 723-733
50. Novick, P., Field, C., and Schekman, R. (1980) *Cell* **21**, 205-215
51. Brachmann, C. B., Davies, A., Cost, G. J., Caputo, E., Li, J., Hieter, P., and Boeke, J. D. (1998) *Yeast* **14**, 115-132
52. Winzeler, E. A., Shoemaker, D. D., Astromoff, A., Liang, H., Anderson, K., Andre, B., Bangham, R., Benito, R., Boeke, J. D., Bussey, H., Chu, A. M., Connelly, C., Davis, K., Dietrich, F., Dow, S. W., El Bakkoury, M., Foury, F., Friend, S. H., Gentalen, E., Giaever, G., Hegemann, J. H., Jones, T., Laub, M., Liao, H., Liebundguth, N., Lockhart, D. J., Lucau-Danila, A., Lussier, M., M'Rabet, N., Menard, P., Mittmann, M., Pai, C., Rebischung, C., Revuelta, J. L., Riles, L., Roberts, C. J., Ross-MacDonald, P., Scherens, B., Snyder, M., Sookhai-Mahadeo, S., Storms, R. K., Véronneau, S., Voet, M., Volckaert, G., Ward, T. R., Wysocki, R., Yen, G. S., Yu, K., Zimmermann, K., Philippsen, P., Johnston, M., and Davis, R. W. (1999) *Science* **285**, 901-906

FOOTNOTES

*This work was supported by a Grant-in-Aid for Young Scientists (A) (17687011) from the Ministry of Education, Culture, Sports, Sciences and Technology of Japan.

[1]Both authors contributed equally to this work

[2]To whom correspondence should be addressed. Tel: +81-11-706-3971; Fax: +81-11-706-4986; E-mail: kihara@pharm.hokudai.ac.jp

[3]The abbreviations used are: LCB, long-chain base; S1P, sphingosine 1-phosphate; LCBP, long-chain base 1-phosphate; MVB, multivesicular body; ER, endoplasmic reticulum; PM, plasma membrane; EGFP, enhanced green fluorescent protein; PAM, plasma membrane associated membrane.

ACKNOWLEDGEMENTS

We thank Dr. R. Schekman (University of California at Berkeley, Berkeley, CA) for providing yeast strains, Dr. J. H. Hegemann (Heinrich-Heine University, Düsseldorf, Germany) for plasmids, Dr. T. Yoshihisa (Nagoya University, Nagoya, Japan) for antiserum, and Dr. E. A. Sweeney for scientific editing and preparation of the manuscript.

FIGURE LEGENDS

FIGURE 1. **Lcb4 is localized in the ER and the PM.** *A*, SEY6210 (wild-type) cells, SIY03 (Δ*lcb4*) cells, and SEY6210 cells bearing pWK79 (*LCB4,* 2 μ) were fixed with formaldehyde, converted to spheroplasts, and permeabilized with 0.1% Triton X-100. Cells were stained with anti-Lcb4, anti-Pma1 (PM marker), or anti-Kar2 (ER marker) antibodies, then observed by fluorescence microscopy. *cER*, cortical ER; *nER*, nuclear ER; *Scale bar*, 5 μm. *B* and *C*, Total cell lysates prepared from SEY6210 cells (*B*) or SEY6210 cells bearing pWK78 (*LCB4, CEN*) (*C*) were fractionated by sucrose gradient centrifugation. Samples were collected from the top (fraction 1) to the bottom (fraction 10) of the gradient. Proteins were separated by SDS-PAGE and subjected to immunoblotting with anti-Lcb4, anti-Dpm1 (ER marker), or anti-Pma1 (PM marker) antibodies.

FIGURE 2. **Lcb4 is localized in the cortical ER and not in the nuclear ER.** *A*, The ultrastructure of SEY6210 (wild-type) cells was examined by electron microscopy. *B* and *C*, SEY6210 cells bearing pWK81 (*LCB4,* 2 μ) (*B*) and SEY6210 parent cells (*C*) were subjected to immunoelectron microscopy using anti-Lcb4 antibodies and 10 nm colloidal gold-conjugated goat anti-rabbit IgG. The *open* and *closed arrows* identify the nuclear ER and the cortical ER, respectively. The *closed arrowheads* indicate the cortical ER-localized Lcb4. *N*, nucleus; *V*, vacuole.

FIGURE 3. **Lcb4 is transported from the Golgi apparatus to the PM via the late Sec pathway.** *A*, SEY6210 (wild-type) cells and the late Sec pathway-defective TS335 (*sec1-1*) cells harboring pUG34 (*EGFP*-vector) or pWK63 (*EGFP-LCB4*), were grown to log phase at 23˚C in SC medium lacking histidine. To induce the expression of EGFP-Lcb4, the culture media were replaced with SC medium lacking both histidine and methionine, and the cells were immediately transferred to 37˚C or kept at 23˚C for 2 h. Cells were fixed with

formaldehyde and observed under a fluorescence microscope. *B*, SEY6210 (wild-type) and TS335 (*sec1-1*) cells, grown at 23˚C to log phase, were pulse-labeled with [^{35}S]methionine/cysteine for 15 min at 23˚C or 37˚C, then chased with excess unlabeled methionine (final concentration of 0.5 mg/ml) and cysteine (final concentration of 0.1 mg/ml) for 0, 1, 2 and 3 h at their respective temperatures. At each time point, lysates were prepared and subjected to immunoprecipitation using anti-Lcb4 antibodies. Immunoprecipitated proteins were separated by SDS-PAGE and detected by autoradiography. *p-Lcb4*, phosphorylated Lcb4.

FIGURE 4. **Lcb4 is transported from the ER to the vacuole via the Golgi/MVB pathway.** (*A*-*C*) Wild-type and mutant cells were grown in YPD medium, then aliquots of cells (2 x 10^7) were harvested and lysed as indicated. Total cell lysates (10 μg protein) were separated by SDS-PAGE, followed by immunoblotting with anti-Lcb4 antibodies. *p-Lcb4*, phosphorylated Lcb4. *A*, RSY255 (wild-type) cells and the early Sec pathway-deficient RSY263 (*sec12-4*) and RSY281 (*sec23-1*) cells were grown at 23˚C until just prior to entering the stationary phase. At time 0, the cultures were shifted to 37˚C, and an aliquot of cells was collected at each indicated time point. *B*, BY4741 (wild-type) cells and cells with deletions in genes affecting endocytosis, including 3033 (Δ*sla1*), 4572 (Δ*chc1*), and 4797 (Δ*clc1*) cells, were grown at 30˚C, then harvested in early log-phase (*E*) or 16 h after reaching stationary phase (*S*). *C*, BY4741 (wild-type) cells and cells with deletions in genes affecting the late Golgi-to-MVB pathway, including SIY259 (Δ*pep12*) and 4462 (Δ*vps45*) cells, were grown at 30˚C, and harvested in early log-phase (*E*) or 16 h after reaching stationary phase (*S*). *D*, BY4741 (wild-type) cells harboring pUG34 (*EGFP*-vector), and BY4741 (wild-type), 4462 (Δ*vps45*) and SIY259 (Δ*pep12*) cells, each harboring pWK63 (*EGFP-LCB4*) were grown to log phase at 30˚C in SC medium lacking histidine. The expression of EGFP and EGFP-Lcb4 was then induced by changing the medium to SC medium lacking both histidine and methionine. The subcellular localization of EGFP-Lcb4 was examined under a fluorescence microscope at 3 h post-induction (log phase) or 24 h post-induction (stationary phase).

FIGURE 5. **G_1 cell cycle arrest triggers degradation of Lcb4.** (*A* and *B*) Cells were grown at 30˚C in YPD medium to a density of 2.0 A_{600}, then treated accordingly. At the indicated time, an aliquot of cells (2 x 10^7) was collected, and the cells were lysed. Total cell lysates (10 μg protein) were separated by SDS-PAGE, followed by immunoblotting with anti-Lcb4 antibodies. *A*, BY4741 (wild-type) cells treated with dimethyl sulfoxide (control) or a cell cycle inhibitor, rapamycin (200 ng/ml; G_1 phase), nocodazole (15 μg/ml; M phase) or hydroxyurea (100 mM; S phase). *B*, 1408 (Δ*bar1*) cells treated with dimethyl sulfoxide (control) or α-factor (6 μg/ml), a G_1 cell cycle inhibitor.

FIGURE 6. **A model for the transport of Lcb4 in log phase and stationary phase.** Lcb4 is synthesized in the cytosol, palmitoylated at the Golgi apparatus (pathway 1), then transported to the PM via the late Sec pathway (pathway 2). Most of the Lcb4 is delivered further to the cortical ER (pathway 3), which is closely adjacent to the PM. Upon reaching the stationary phase, the ER-localized Lcb4 is transported to the Golgi apparatus via the early Sec pathway (pathway 4), and finally to the vacuole, via the MVB pathway (pathway 5 and 6).

TABLE 1. *Yeast strains used in this study*

Strain	Genotype	Source
SEY6210	*MATα leu2-3,112 ura3-52 his3-Δ200 trp1-Δ901 lys2-801 suc2-Δ9*	Ref. 48
SIY03	SEY6210, Δ*lcb4::TRP1*	Ref. 9
RSY255	*MATα leu2-3,112 ura3-52*	Ref. 49
RSY263	RSY255, *sec12-4*	Ref. 49
RSY281	RSY255, *sec23-1*	Ref. 49
HMSF1	*MATα sec1-1*	Ref. 50
TS335	*MATα leu2-3,112 ura3-52 his3-Δ200 trp1-Δ901 lys2-801 suc2-Δ9 sec1-1*	This study
BY4741	*MAT**a** his3Δ1 leu2Δ0 met15Δ0 ura3Δ0*	Ref. 51
1408	BY4741, Δ*bar1::KanMX4*	Ref. 52
3033	BY4741, Δ*sla1::KanMX4*	Ref. 52
4462	BY4741, Δ*vps45::KanMX4*	Ref. 52
4572	BY4741, Δ*chc1::KanMX4*	Ref. 52
4797	BY4741, Δ*clc1::KanMX4*	Ref. 52
SIY259	BY4741, Δ*pep12::LEU2*	This study

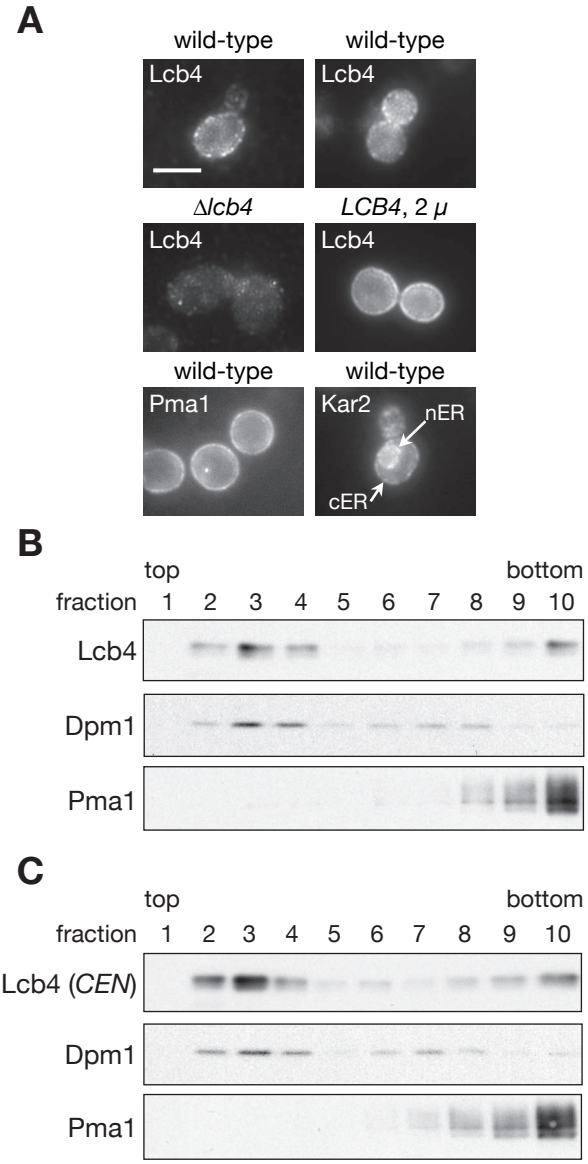

Iwaki *et al.*, Fig. 1

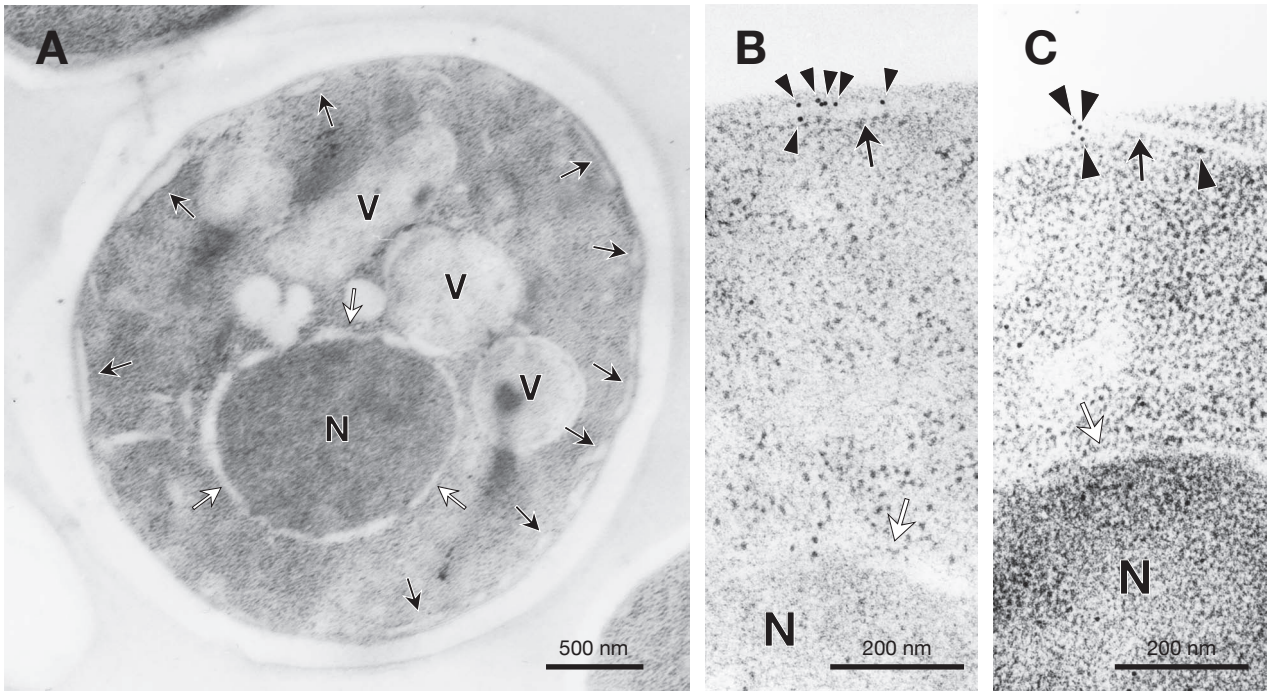

Iwaki *et al.*, Fig. 2

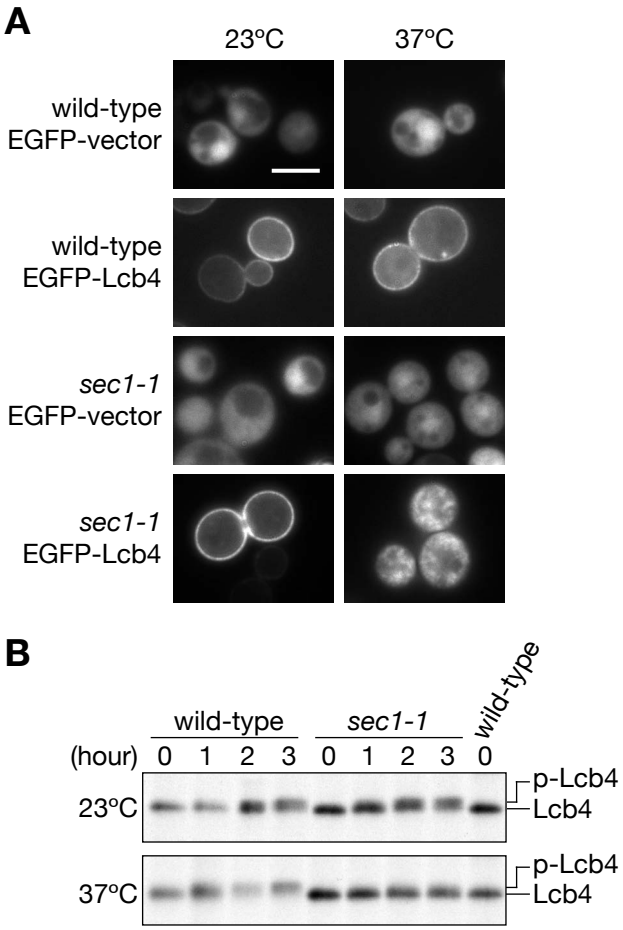

Iwaki *et al.*, Fig. 3

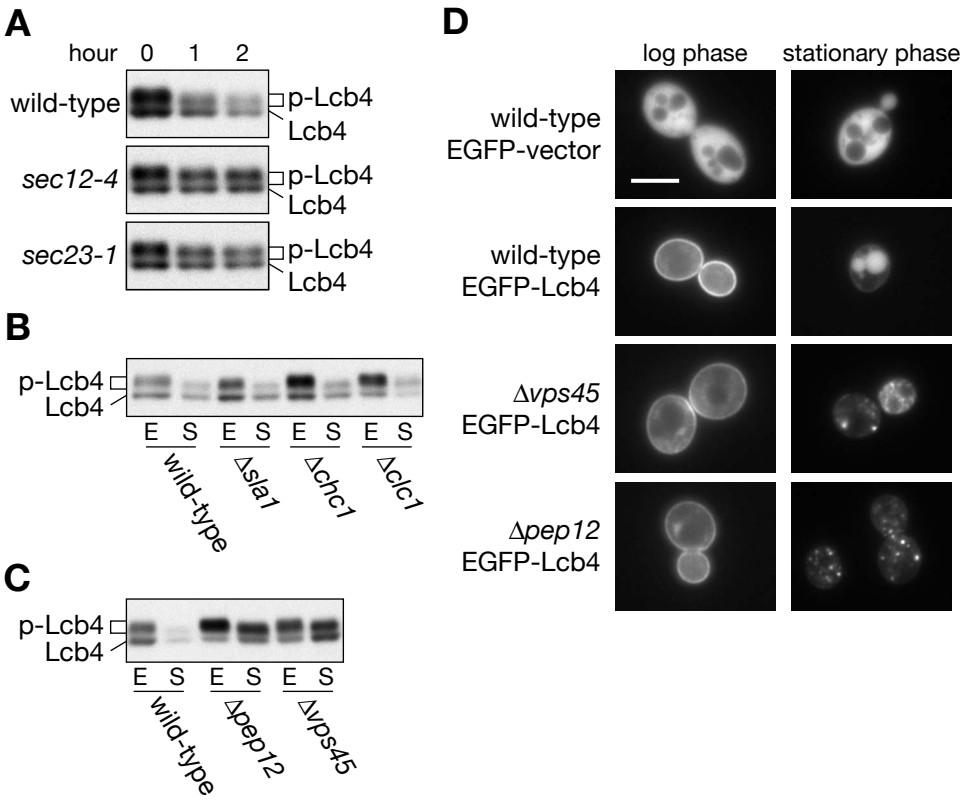

Iwaki *et al.*, Fig. 4

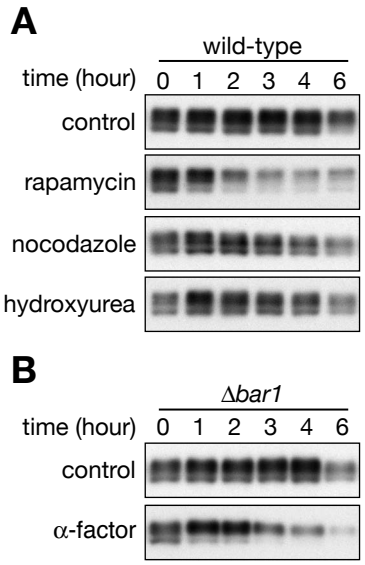

Iwaki *et al.*, Fig. 5

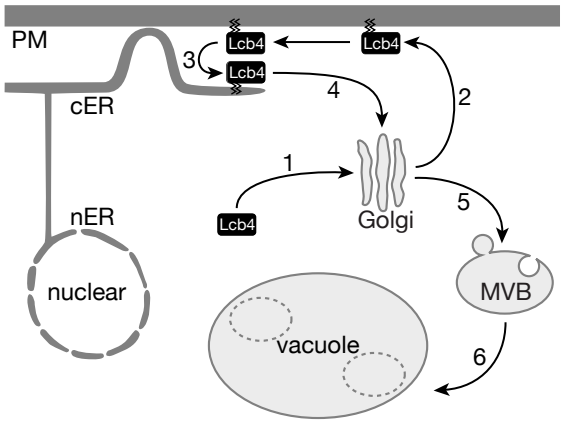

Iwaki *et al.*, Fig. 6